

## Supporting Information

### Electrostatic swelling of bicontinuous cubic lipid phases

*A.I.I. Tyler, H.M.G. Barriga, E.S. Parsons, N.L.C. McCarthy, O. Ces, R.V. Law, J.M. Seddon and N.J. Brooks*

#### S1. Materials and methods

1,2-dioleoyl-sn-glycero-3-phospho(1'-rac-glycerol) (sodium salt) (DOPG) and 1,2-dioleoyl-sn-glycero-3-phospho-L-serine (sodium salt) (DOPS) were purchased from Avanti Polar Lipids (AL, USA). Cholesterol (CHOL) and 1-Oleoyl-rac-glycerol (Monoolein, MO) were purchased from Sigma Aldrich (Gillingham, UK). The lipids had a purity of >99% and were used without further purification. Each lipid was freeze-dried individually and samples were then prepared by mixing appropriate amounts of dry lipids and co-dissolving them in chloroform. They were subsequently vortexed, dried under a steam of nitrogen gas and lyophilised for a minimum of 24 h. Samples were hydrated in HPLC grade water (VWR, UK) to a minimum of 70 wt% water and subjected to at least 20 freeze-thaw cycles between -210 and 40 °C, and a minimum of 5 pressure cycles (1 to 2000 bar)<sup>1</sup> in order to homogenize the mixtures. The water content (70wt%) was the maximum where it was still possible to obtain clear diffraction patterns.

X-ray experiments were carried out on beamline ID02 at the European Synchrotron Radiation Facility (ESRF) and I22 at Diamond Light source (DLS). The synchrotron X-ray beam was tuned to a wavelength of 0.73 Å (ESRF) or 0.69 Å (DLS). The distance between the sample and detector was set at 1.2 m, 1.5m, 3.0m, 4.0m or 4.5m and the 2-D powder diffraction patterns were recorded on an image-intensified FReLoN Kodak CCD (ESRF) or Pilatus 2M (DLS) detector. Silver behenate ( $a = 58.38 \text{ \AA}$ ) was used to calibrate the small-angle X-ray diffraction data for all measurements. Diffraction images were analyzed using the IDL-based AXcess software package, developed by Dr A. Heron.<sup>2</sup>

Water volume fraction calculations were carried out using Mathematica (Mathematica 7.5, Wolfram Research Inc.).

#### S2. Structural models for bicontinuous cubic phases

Two geometric models have been established to describe the bicontinuous cubic phases, the parallel interface model (PIM) and the constant mean curvature model (CMCM).<sup>3</sup> The PIM (where the hydrophilic – hydrophobic interface of each monolayer lies parallel to the underlying periodic minimal surface) predicts that the three bicontinuous cubic structures can be interconverted through the Bonnet transformation,<sup>4</sup> which is a mathematical procedure involving surface patches being continuously bent into each other whilst preserving the curvatures, angles, distances and areas on the surface. The lattice parameters ( $a$ ) for the Bonnet related cubic phases should have the ratio  $a_{\text{Im}3\text{m}} : a_{\text{Pn}3\text{m}} : a_{\text{Ia}3\text{d}} = 1.279 : 1.000 : 1.576$ . The PIM suggests that the three bicontinuous cubic phases are energetically degenerate; however these phases have been stably isolated in numerous experimental studies. In the CMCM model (where the interfaces have a constant mean curvature which requires some elongation and compression of the lipid hydrocarbon chains moving laterally across the bilayer) the degeneracy is broken and it predicts that these phases will appear in the order of Ia3d – Pn3m – Im3m upon increasing hydration.<sup>3</sup>

The ratio between the lattice parameters of the coexisting Im3m and Pn3m phases observed in MO:CHOL mixtures with more than 15 mol% CHOL was found to be 1.29, which is very

close to the theoretical Bonnet ratio of 1.279. It should be noted that the existence of the Im3m phase has been questioned in favor of a cubic phase based on the I-WP surface.<sup>5</sup> However the theoretical  $a_{I-WP} : a_{Pn3m}$  ratio is 1.82, which is very different from the ratio found in these experiments.

### S3. Calculations of water volume fraction using the PIM and CMCM models

By using the PIM and CMCM models we can calculate the water volume fraction of the mesophase from the experimentally determined lattice parameter to determine if the samples are coexisting with excess water. As the molecular parameters required for the calculations are not available for binary or ternary mixtures of MO, we have used values for pure MO as an approximation.

The water volume fractions calculated from the experimentally determined lattice parameters using the PIM and CMCM are very close (within 3%) and so only the CMCM values are considered.

The lattice parameter is related to the water volume fraction as shown in equations S1 and S2 for the PIM and CMC models respectively:

$$a_{PIM} = \frac{V_n}{A_n(1-\varphi_w)} \left( -2\sigma + \frac{2^{\frac{5}{3}}\sigma^2}{\left(4\sigma^3 + 9\pi\chi(1-\varphi_w)^2\left(\frac{V_n}{V}\right)^2 + 3(1-\varphi_w)\left(\frac{V_n}{V}\right)\sqrt{\pi\chi(8\sigma^3 + 9\pi\chi(1-\varphi_w)^2\left(\frac{V_n}{V}\right)^2)}\right)^{\frac{1}{3}}} + 2^{\frac{1}{3}} \left(4\sigma^3 + 9\pi\chi(1-\varphi_w)^2\left(\frac{V_n}{V}\right)^2 + 3(1-\varphi_w)\left(\frac{V_n}{V}\right)\sqrt{\pi\chi(8\sigma^3 + 9\pi\chi(1-\varphi_w)^2\left(\frac{V_n}{V}\right)^2)}\right)^{\frac{1}{3}} \right) \quad (S1)$$

$$a_{CMC} = 2 \sum_i \frac{\sigma_i \left[ \left( \frac{V_n}{V} \right) (1-\varphi_w) \right]^{2i}}{\left( \frac{A_n}{V} \right) (1-\varphi_w)} \quad (S2)$$

Where:

$a$  is the lattice parameter

$V_n$  is the volume between the minimal surface and the pivotal surface

$A_n$  is the area at the pivotal surface

$V$  is the molecular volume

$\varphi_w$  is the water volume fraction

$\sigma$  is the dimensionless surface area

$\chi$  is the Euler characteristic (-4 for the Im3m phase and -2 for the Pn3m phase)

$\sigma_i$  is the calculated dimensionless surface area for the CMCM.

The water volume fraction ( $\varphi_w$ ) is given by:

$$\varphi_w = \frac{C_w}{C_w + \left( (1-C_w) \left( \frac{\rho_w}{\rho_l} \right) \right)} \quad (S3)$$

Where:

$C_w$  is the wt% water

$\rho_l$  is the density of the lipid

$\rho_w$  is the density of water

For the CMCM model, the values of  $A_n$ ,  $V_n$  and  $V$  for MO were used<sup>6</sup> with  $\sigma_i$  for both the Pn3m and Im3m phases.<sup>3</sup> Values for  $A_n$  and  $V_n$  for the PIM model were taken from calculations for MO in the Ia3d phase at 25°C as shown in Table S1 below.<sup>7</sup>

**Table S1.** Structural parameters used for the PIM and CMCM model calculations

Molecular Parameter	PIM (Pn3m)	PIM (Im3m)	CMCM (Pn3m)	CMCM (Im3m)
$V_n / \text{\AA}^3$	451	451	465	465
$A_n / \text{\AA}^2$	32.6	32.6	33	33
$V / \text{\AA}^3$	612	612	612	612
$\sigma$	1.9189	2.3451		
$\sigma_0$			1.9189	2.3451
$\sigma_1$			-0.8893	-1.1713
$\sigma_2$			-0.061856	-0.22227
$\sigma_3$			-0.65474	-2.4952

#### S4. Spontaneous curvature of charged phospholipids

The spontaneous curvature of charged lipids is likely to change significantly as a function of the ionic strength and pH of their aqueous environment.  $H_0$  has been calculated for DOPS ( $1/144 \text{\AA}^{-1}$  buffered at pH 7),<sup>8</sup> DOPG ( $-1/1500 \text{\AA}^{-1}$  in 150mM NaCl, pH 7)<sup>9</sup> and DOPA ( $-1/46 \text{\AA}^{-1}$  in 150mM NaCl, pH 7)<sup>10</sup> mixtures. A more negative  $H_0$  favors formation of structures with larger inverse curvature and so it appears that DOPA should promote the most negative curvature, followed by DOPG and finally DOPS. However, the  $H_0$  of DOPA is known to change significantly in pure water to  $-1/130 \text{\AA}^{-1}$ .<sup>10</sup> DOPS has a large positive  $H_0$  value at neutral pH and so when confined to a flat membrane will tend to reduce the lateral pressure in the hydrophobic region of the bilayer. This is analogous to LysoPC which can hinder or encourage different intermediate stages in membrane fusion depending on its location.<sup>11</sup> Interestingly, at low pH and without the addition of salt, DOPS transforms from a lamellar to an  $H_{II}$  phase<sup>12</sup> and its  $H_0$  value changes drastically to  $-1/23 \text{\AA}^{-1}$  at pH 2. This is even more negative than the archetypal non-lamellar forming lipid DOPE ( $-1/30 \text{\AA}^{-1}$ ).<sup>8</sup> The  $pK_a$  of the carbonyl carboxyl group of the DOPS headgroup is estimated to be approximately 4.3<sup>13</sup> and the apparent  $pK_a$  of 20% DOPS in MO has been estimated to be 2.5<sup>14,15</sup> so the significant change in behavior at pH 2 is likely to be related to protonation of this group.

It is also known that phosphatidylserine lipids can form hydrogen bond networks<sup>16,17</sup> resulting in a much smaller area per lipid than found for equivalent phosphatidylcholine lipids. Both DOPS and DOPG have three sites in their headgroup that can hydrogen bond to neighboring lipids (both to charged lipids and MO) and their propensity to do so has been confirmed experimentally.<sup>18,19</sup> This hydrogen bonded network will result in a reduction in the effective headgroup size, a lateral condensing of the bilayer and a decreased hydration of the headgroup which will increase the magnitude of  $H_0$ . However, the net charge on the phospholipid will create an electrostatic attraction between the headgroup and the dipole moment of surrounding water molecules, which will result in attraction of water molecules near to the headgroup, increasing its net volume and hence making  $H_0$  more positive. These interconnected effects make it very difficult to predict *a priori* the effect of doping MO with different charged phospholipids.

## S5. Results

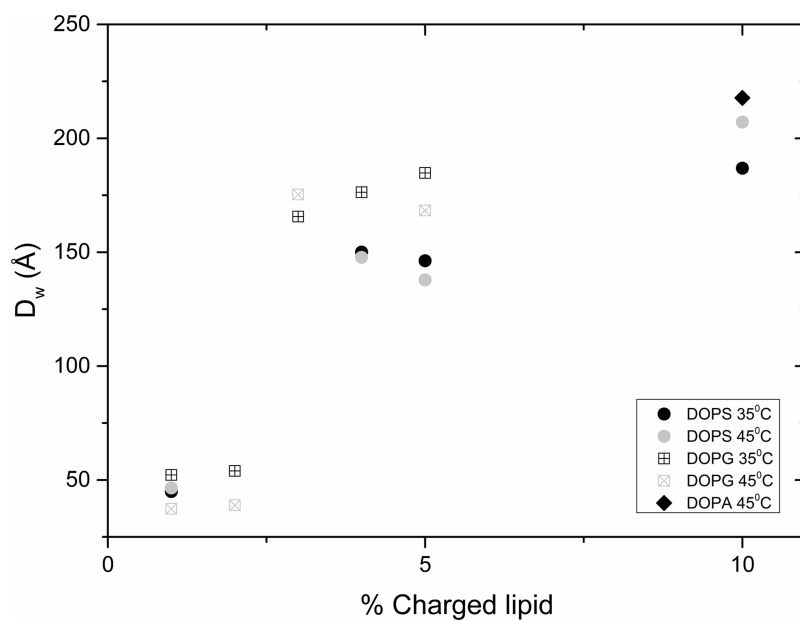


**Figure S1.** Calculated water channel diameters for the Im3m cubic phase of MO with increasing amount of the anionic lipids DOPS, DOPG and DOPA.

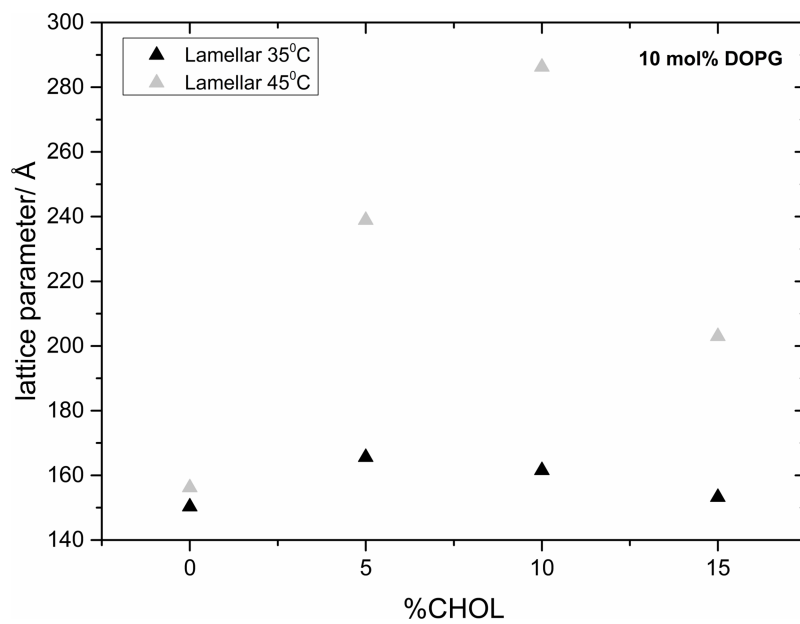


**Figure S2.** Phase behaviour and effect on the lattice parameter of incorporating CHOL into MO:DOPG mixtures keeping the DOPG concentration constant at 10 mol%.

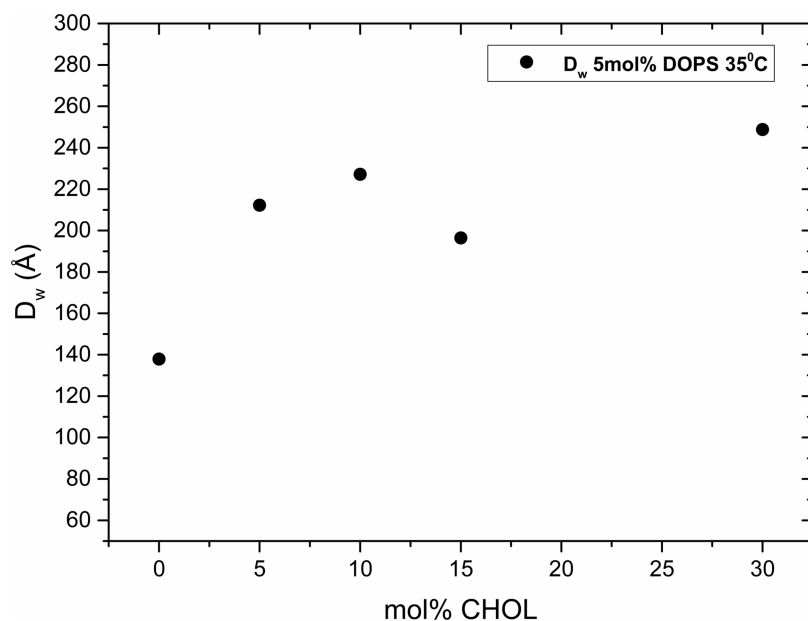


**Figure S3.** Calculated water channel diameters for the Im3m cubic phase of MO with 5 mol% DOPS and increasing amounts of CHOL.

### Supporting Information References

- (1) Brooks, N. J.; Gauthe, B. L. L. E.; Terrill, N. J.; Rogers, S. E.; Templer, R. H.; Ces, O.; Seddon, J. M. *Rev Sci Instrum* **2010**, *81*.
- (2) Seddon, J. M.; Squires, A. M.; Conn, C. E.; Ces, O.; Heron, A. J.; Mulet, X.; Shearman, G. C.; Templer, R. H. *Philos T R Soc A* **2006**, *364*, 2635.
- (3) Templer, R. H.; Seddon, J. M.; Duesing, P. M.; Winter, R.; Erbes, J. *J Phys Chem B* **1998**, *102*, 7262.
- (4) Hyde, S. T. *J Phys Chem-Us* **1989**, *93*, 1458.
- (5) Luzzati, V. *J Phys li* **1995**, *5*, 1649.
- (6) Shearman, G. C.; Khoo, B. J.; Motherwell, M. L.; Brakke, K. A.; Ces, O.; Conn, C. E.; Seddon, J. M.; Templer, R. H. *Langmuir* **2007**, *23*, 7276.
- (7) Templer, R. H. *Langmuir* **1995**, *11*, 334.
- (8) Fuller, N.; Benatti, C. R.; Rand, R. P. *Biophys J* **2003**, *85*, 1667.
- (9) Alley, S. H.; Ces, O.; Barahona, M.; Templer, R. H. *Chem Phys Lipids* **2008**, *154*, 64.
- (10) Kooijman, E. E.; Chupin, V.; Fuller, N. L.; Kozlov, M. M.; de Kruijff, B.; Burger, K. N. J.; Rand, P. R. *Biochemistry-Us* **2005**, *44*, 2097.
- (11) Chernomordik, L.; Chanturiya, A.; Green, J.; Zimmerberg, J. *Biophys J* **1995**, *69*, 922.
- (12) Bezrukov, S. M.; Rand, R. P.; Vodyanoy, I.; Parsegian, V. A. *Faraday Discuss* **1998**, *111*, 173.
- (13) Dekroon, A. I. P. M.; Timmermans, J. W.; Killian, J. A.; Dekruiff, B. *Chem Phys Lipids* **1990**, *54*, 33.
- (14) Okamoto, Y.; Masum, S. M.; Miyazawa, H.; Yamazaki, M. *Langmuir* **2008**, *24*, 3400.
- (15) Oka, T.; Tsuboi, T.; Saiki, T.; Takahashi, T.; Alam, J. M.; Yamazaki, M. *Langmuir* **2014**, *30*, 8131.
- (16) Petrache, H. I.; Tristram-Nagle, S.; Gawrisch, K.; Harries, D.; Parsegian, V. A.; Nagle, J. F. *Biophys J* **2004**, *86*, 1574.
- (17) Miller, I. R.; Eisenstein, M. *Bioelectrochemistry* **2000**, *52*, 77.
- (18) Lewis, R. N. A. H.; McElhaney, R. N. *Biophys J* **2000**, *79*, 2043.
- (19) Razumas, V.; Talaikyte, Z.; Barauskas, J.; Larsson, K.; Mieziš, Y.; Nylander, T. *Chem Phys Lipids* **1996**, *84*, 123.